ELSEVIER

Electroless synthesis of large scale Co–Zn–P nanowire arrays and the magnetic behaviour

Xiaoyou Yuan [a,b,*], Chunsheng Du [a], Gang Sun [a], Ning Pan [a]

[a] Nanomaterials in the Environment, Agriculture, and Technology, University of California, Davis, CA 95616, United States
[b] Department of Chemistry, Anhui University, Hefei 230039, PR China

Abstract

Co–Zn–P nanowire arrays have been synthesized by electroless deposition in an anodic alumina membrane (AAM). The images of Co–Zn–P nanowire arrays and single nanowires are obtained by both scanning electron microscope (SEM) and transmission electron microscope (TEM), respectively. Selected area electron diffraction (SAED), X-ray diffraction (XRD) and energy dispersive spectra (EDS) are employed to study the morphology and chemical composition of the nanowires. The results indicate that Co–Zn–P nanowire arrays are amorphous in structure. The hysteresis loops characterized by a vibrating sample magnetometer (VSM) show that the easily magnetized direction of Co–Zn–P nanowire arrays is parallel to the nanowire arrays and that there exhibits clearly a magnetic anisotropy as a result of the shape anisotropy.
© 2006 Elsevier B.V. All rights reserved.

1. Introduction

Fabrication of magnetic nanowire arrays has become the subject of intensive study [1–4] due to their potential applications in ultra-high-density magnetic storage devices and microsensors [5]. The properties and applications of magnetic nanowire arrays arise from their inherent shape anisotropy and the low dimension. Magnetic nanowire arrays as an ultra-high-density magnetic storage material can achieve recoding densities of more than 100 Gbit/in.^{2}, beyond the predicted thermal limits of 40 Gbit/in.^{2} in continuous magnetic film [6,7].

To meet ultra-high-density magnetic recording, research has focused on the fabrication of perpendicular anisotropy magnetic nanowire arrays. But in some cases (such as Co, Ni nanowires), due to the competition between magnetocrystalline anisotropy and shape anisotropy, there may be no

perpendicular anisotropy [8,9]. Since the magnetic properties are related to element components and morphology of material, the perpendicular anisotropy can be adjusted by mixing different chemical element to form alloy, ternary alloy amorphous magnetic nanowire arrays may be candidate to exhibit the perpendicular anisotropy.

There have been reports of fabrication of single element and binary alloy magnetic nanowire arrays by electrodeposition in AAM [10–14]. However, ternary alloy magnetic nanowire arrays have not been reported so far. Because the redox evolution potential and kinetic behaviour of these elements are different, it is very difficult to electrodeposit simultaneously ternary alloy nanowire arrays of uniform on a large-scale in an aqueous solution, especially the difference of standard electrode potential among these elements is larger.

With adequate efforts however, we have finally succeeded in fabricating Co–Zn–P alloy nanowire arrays on a large-scale with electroless deposition in AAM. Compared with the electrodeposition method, electroless deposition method requires neither a supply of power nor a sprinkling of gold (Au, as a conductive layer) on one side of the AAM before the deposition process, which is carried out via a redox reaction involving an oxidizer and a reductant in an electrolyte solution

* Corresponding author at: Nanomaterials in the Environment, Agriculture, and Technology, University of California, Davis, CA 95616, United States. Fax: +530 752 7584.
  E-mail address: xyyuan@ucdavis.edu (X.Y. Yuan).

[15–17]. It is an autocatalytic self-assembly process, can be promised for the production of uniform nanowire arrays on a large-scale, and more importantly, will make it possible to control the aspect ratio of the nanowire using AAM of chosen pore size and thicknesses. Control of the uniform in size and shape of nanowire arrays on a large-scale is recognized as a very important issue in the fabrication of nanostructure [18–20], and turned out to be a challenging problem [21–24].

2. Experimental

The AAM template was prepared following the procedure described by Masuda and Fukuda [25]. The pores of the AAM template were about 70 nm in diameter and 5 μm in depth with interpore spacing of 100 nm. The through-hole AAM template was first immersed in an aqueous solution of $SnCl_2$ (10 g l^{-1}) for 1 min and washed with distilled water two to three times, and then, the AAM template was further kept in a solution of $PdCl_2$ (1 g l^{-1}) for 30 s and rinsed with distilled water several times again. Subsequently, Co–Zn–P nanowire arrays were deposited in the pores of the AAM from a solution of 15 g l^{-1} $CoCl_2 \cdot 6H_2O$, 2 g l^{-1} $ZnSO_4$, 20 g l^{-1} $NaH_2PO_2 \cdot H_2O$, and 50 g l^{-1} Rochelle salt at 80–85 °C, the pH of the solution is about 9.0 adjusted by ammonia, the deposition time is 5 min.

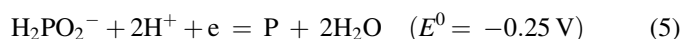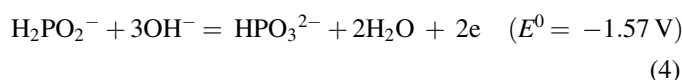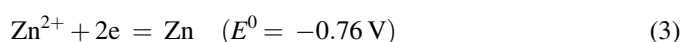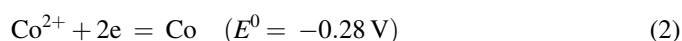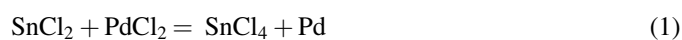In order to isolate the Co–Zn–P nanowire arrays, the AAM with the Co–Zn–P nanowire arrays was dissolved in 5 wt% NaOH solution at 25 °C for 5 min and slightly washed several times with distilled water to remove the dissolved AAM and the remaining NaOH solution. For the scanning electron microscope (SEM, JSM-6700F) images, the above Co–Zn–P nanowire arrays were directly mounted on the Cu stubs with a conductive gold paint. The sample for the transmission electron microscope (TEM, H-800) was treated with a 5 wt% NaOH solution for 10 min and dispersed in alcohol. Then a small drop of the solution was placed on a carbon film supported by Cu grids.

Selected area electron diffraction (SAED), energy dispersive spectra (EDS, TEM JEOL-2010) and X-ray diffraction with Cu Kα radiation (XRD, MXP18AHF) were employed to study the morphology and chemical composition of the nanowires. The magnetic property of Co–Zn–P alloy nanowire arrays was characterized using a vibrating sample magnetometer (VSM, BHV-55), with the applied magnetic field parallel and then perpendicular to nanowire arrays to examine the magnetic behaviour.

3. Results and discussion

Fig. 1 shows a SEM image of the Co–Zn–P alloy nanowire arrays prepared by electroless deposition in an AAM. Fig. 1a is the view from the top and Fig. 1b is the view from the side. Fig. 1a indicates that the Co–Zn–P alloy nanowire arrays are uniform, and all pores of in the AAM are filled up. Fig. 1b reveals that the nanowires, about 3 μm in length, are parallel to each other. The SEM images reveal that the Co–Zn–P nanowire arrays fabricated by electroless deposition are uniform on a large-scale. The reactions in the fabrication of Co–Zn–P nanowire arrays are as follows

$$SnCl_2 + PdCl_2 = SnCl_4 + Pd \tag{1}$$

$$Co^{2+} + 2e = Co \quad (E^0 = -0.28\,V) \tag{2}$$

$$Zn^{2+} + 2e = Zn \quad (E^0 = -0.76\,V) \tag{3}$$

$$H_2PO_2^- + 3OH^- = HPO_3^{2-} + 2H_2O + 2e \quad (E^0 = -1.57\,V) \tag{4}$$

$$H_2PO_2^- + 2H^+ + e = P + 2H_2O \quad (E^0 = -0.25\,V) \tag{5}$$

E^0 represents standard single electrode potential. If E^0 value of a reductant is lower than that of an oxidizer, the reaction between an oxidizer and a reductant will be possible to take place in the view of thermodynamics. The larger the electrode potential difference between an oxidizer and a reductant, the higher the possibility of redox reaction. According to the E^0 values, Co, Zn and P could be reduced by NaH_2PO_2 in the alkaline electrolyte solution. However, these reactions among Eqs. (2)–(5) cannot take place without the presence of some catalyst, which is controlled by kinetics. Pd atoms act as a catalyst in the reactions.

The growth mechanism of the Co–Zn–P nanowire arrays is as follows: first, $SnCl_2$ solution adhered to the pore walls in the AAM hydrolyzes to form $Sn(OH)_2$ in the aqueous solution. Then, $PdCl_2$ is reduced to Pd atoms by $Sn(OH)_2$, and the Pd atoms trigger the redox reactions. Once the redox reactions are initiated, the reactions from Eqs. (2)–(5) will be autocatalyzed.
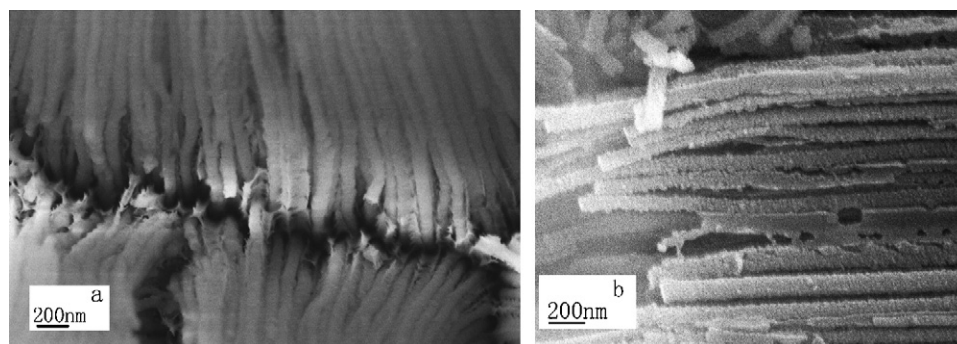

Fig. 1. SEM images of Co–Zn–P nanowire arrays: (a) view from the top and (b) view from the side.
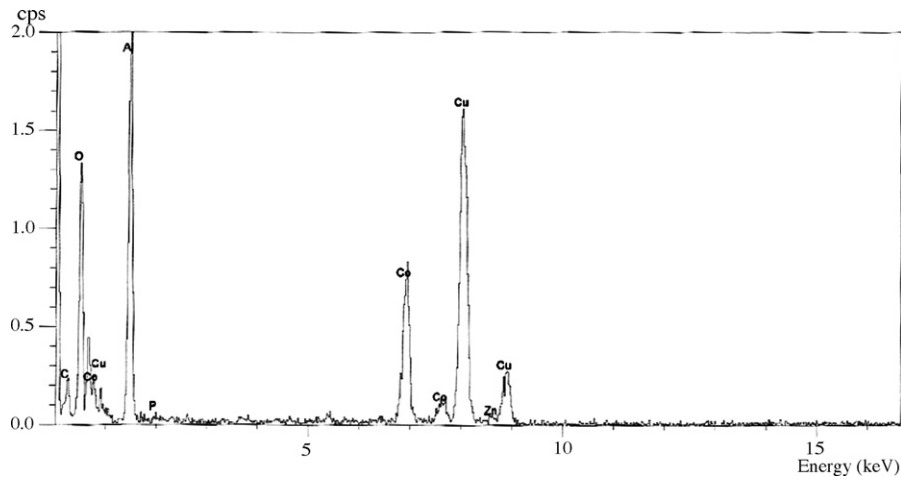
Fig. 2. The EDS of a Co–Zn–P alloy nanowire. The atomic ratio of Co:Zn:P is 95.2:1.5:3.3, the mass percentage of Co:Zn:P is 96.6:1.6:1.8.

In fact, as a catalyst, the concentration of Pd atoms is very low so that no trace of it is seen on the EDS spectrum in Fig. 2.

Since the electroless deposition requires neither a supply of power nor a sprinkling of Au on one side of the AAM before the
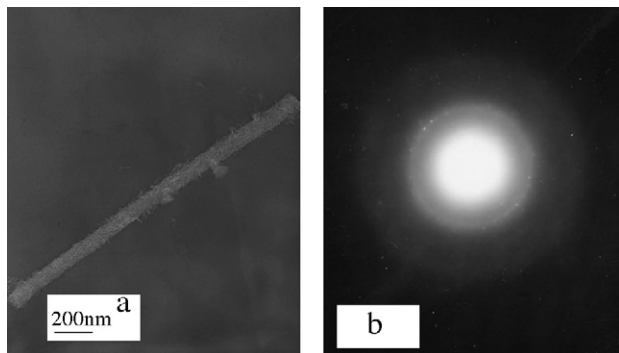

Fig. 3. (a) TEM image of Co–Zn–P alloy nanowires with diameter about 70 nm. (b) SAED of Co–Zn–P alloy nanowire.
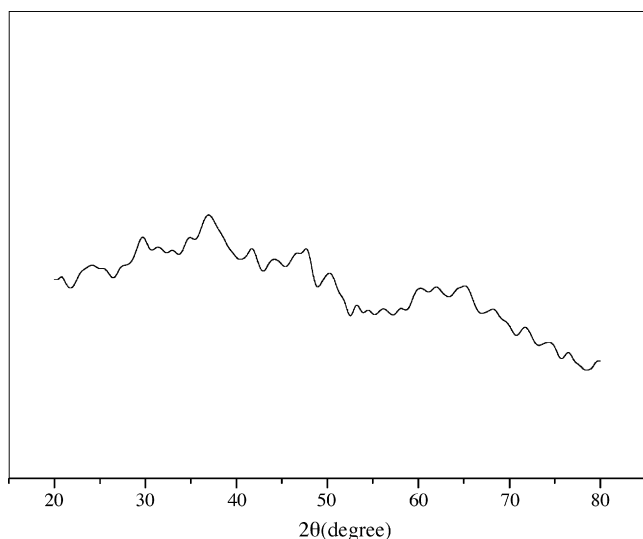

Fig. 4. The X-ray diffraction pattern for Co–Zn–P nanowires.

deposition process, it can avoid some defects of electrodeposition method, just as Prieto et al. described [14]. In the method of electroless deposition, redox reactions are autocatalytic self-assembly process and the electrolyte solution concentration is uniform, Co–Zn–P nanowire arrays are formed where there is the electrolyte solution. The Co–Zn–P nanowire arrays are going to be large-scale and uniform (see Fig. 1 SEM images). The TEM and SAED images of single Co–Zn–P nanowire in Fig. 3 confirms that the Co–Zn–P nanowire is about 70 nm in diameter and 3 μm in length. Fig. 3b reveals that Co–Zn–P nanowire is amorphous in structure, which is confirmed by the XRD spectrum as shown in Fig. 4. This amorphous structure of Co–Zn–P nanowire arrays will meet the need of perpendicular anisotropy in magnetic properties.

The EDS shown in Fig. 2 confirms that the nanowires are composed of Co, Zn and P, the atomic ratio of Co:Zn:P is 95.2:1.5:3.3, the mass percentage of Co:Zn:P is 96.6:1.6:1.8. Fig. 5 is the hysteresis loop of Co–Zn–P nanowire arrays measured at room temperature. The H|| represents the external magnetic field parallel to the Co–Zn–P nanowire arrays, and the $H_\perp$ perpendicular to the Co–Zn–P nanowire arrays. As can be
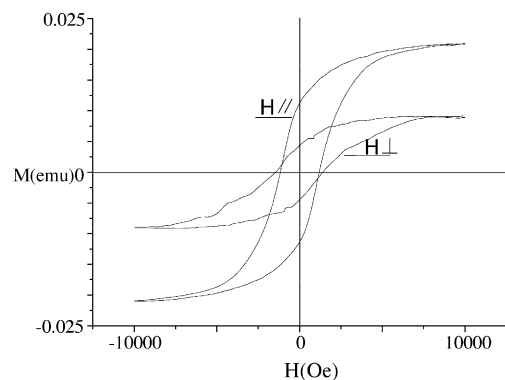

Fig. 5. Hysteresis loops of Co–Zn–P nanowire arrays embedded in AAM at room temperature. The $H_{||}$ represents the direction of magnetic field applied parallel to Co–Zn–P nanowire arrays and the $H_\perp$ perpendicular to Co–Zn–P nanowire arrays.

seen, the values of magnetization (M) that appeared to saturate at 10000 Oe and the remanence (M_r) of $H_{||}$ are both larger than those of $H_\perp$. The coercivities (H_c) of Co–Zn–P nanowire arrays for $H_{||}$ and $H_\perp$ orientation are about 1100 and 1200 Oe, respectively. The hysteresis loops indicate that the easily magnetized direction of Co–Zn–P nanowire arrays is parallel to the nanowire arrays and that it has obvious magnetic anisotropy. We can expect from Figs. 3b and 4 that the competition between shape anisotropy and magnetocrystalline anisotropy is unlikely to occur in the present case, because this latter contribution does not exist due to the amorphous structure of these Co–Zn–P nanowires. The magnetic anisotropy of Co–Zn–P nanowire is a result of the shape anisotropies. It is due to the perpendicular anisotropy that the Co–Zn–P nanowire arrays are a good candidate for ultra-high-density magnetic recoding media.

4. Conclusions

Uniform Co–Zn–P magnetic nanowire arrays have been successfully fabricated on a large-scale by electroless deposition in AAM. The results indicate that the Co–Zn–P nanowire is amorphous in structure. The hysteresis loops show that the easily magnetized direction of Co–Zn–P nanowire arrays is parallel to the nanowire arrays and that it has obvious magnetic anisotropy as a result of the shape anisotropy. Electroless deposition method can be extended to many other materials and opens up significant opportunities in the nanoscale fabrication of magnetic materials for ultra-high-density magnetic recoding.

Acknowledgements

References

[1] W.X. Li, G.A. Jones, P. Yong, T.H. Shena, J. Appl. Phys. 97 (2005) 104306.
[2] A. Ursache, J.T. Goldbach, T.P. Russell, M.I. Tuominena, J. Appl. Phys. 97 (2005) 10J322.
[3] D.H. Qin, H.L. Zhang, C.L. Xu, T. Xu, H.L. Li, Appl. Surf. Sci. 239 (2005) 279.
[4] A.J. Bennett, J.M. Xu, Appl. Phys. Lett. 82 (2003) 3304.
[5] S. Sun, C.B. Murray, D. Weller, L. Folks, A. Moser, Science 287 (2000) 1989.
[6] D. Routkevitch, A.A. Tager, J. Haruyama, D. Almawlawi, M. Moskovits, J.M. Xu, IEEE Trans. Electron. Devices 43 (1996) 1646.
[7] P.L. Lu, S.H. Charap, IEEE Trans. Magn. 30 (1994) 4230.
[8] L. Piraux, S. Dubois, E. Ferain, J. Magn. Magn. Mater. 165 (1997) 352.
[9] P.M. Paulus, F. Luis, M. Kröll, G. Schmid, L.J. de Jongh, J. Magn. Magn. Mater. 224 (2001) 180.
[10] G.J. Strijkers, J.H.J. Dalderop, M.A.A. Broeksteeg, H.J.M. Swagten, W.J.M. deJonge, J. Appl. Phys. 86 (1999) 5141.
[11] S. Park, S. Kim, S. Lee, Z.G. Khim, K. Char, T. Hyeon, J. Am. Chem. Soc. 122 (2000) 8581.
[12] Y.W. Wang, G.W. Meng, C.H. Ling, G.Z. Wang, L.D. Zhang, Chem. Phys. Lett. 343 (2001) 174.
[13] S.G. Yang, H. Zhu, D.L. Yu, Z.Q. Jin, S.L. Tang, Y.W. Du, J. Magn. Magn. Mater. 222 (2000) 97.
[14] A.L. Prieto, M.S. Sander, M.S. Martin, R. Gronsky, T. Sands, A.M. Stacy, J. Am. Chem. Soc. 123 (2001) 7160.
[15] J.L. Gu, J.L. Shi, L.M. Xiong, H.R. Chen, L. Li, M.L. Ruan, Solid State Sci. 6 (2004) 747.
[16] T. Qiu, X.L. Wu, Y.F. Mei, G.J. Wan, P.K. Chu, G.G. Siu, J. Cryst. Growth 277 (2005) 143.
[17] Z.L. Shi, S.Q. Wu, J.A. Szpunar, Chem. Phys. Lett. 422 (2006) 147.
[18] Y.W. Jun, S.M. Lee, N.J. Kang, J. Cheon, J. Am. Chem. Soc. 123 (2001) 5150.
[19] Y.W. Cao, R. Jin, C.A. Mirkin, J. Am. Chem. Soc. 123 (2001) 7961.
[20] F.K. Kim, J.H. Song, P.D. Yang, J. Am. Chem. Soc. 124 (2002) 14316.
[21] C.P. Gibson, K.J. Putzer, Science 267 (1995) 1338.
[22] M.P. Pileni, B.W. Ninham, T.G. Krzywicki, J. Tanori, I. Lisiecki, A. Filankembo, Adv. Mater. 11 (1999) 1358.
[23] M. Li, H. Schnablegger, S. Mann, Nature 402 (1999) 393.
[24] X. Peng, L. Manna, W. Yang, J. Wickham, E. Scher, A. Kadavanich, A.P. Alivisatos, Nature 404 (2000) 59.
[25] H. Masuda, K. Fukuda, Science 268 (1995) 1466.